SLIP CORRELATIONS ON A CREEPING FAULT

Hugo Perfettini and Jean Schmittbuhl
Laboratoire de Geologie, Ecole Normale Superieure, Paris, France

Jean-Pierre Vilotte
Département de Sismologie, Institut de Physique du Globe, Paris, France

Short title: SLIP ON A CREEPING FAULT

Abstract. Using a quasi-static three dimensional fault model which accounts for long range elastic interactions, we examine the influence of spatial heterogeneities of frictional strength on the slip distribution along a creeping fault. Slip fluctuates spatially because of pinning on local asperities. We show that three regimes of slip correlations exist. The first regime results in a uniform slip in an homogeneous medium. On the contrary, slip in the second regime highly fluctuates and is controlled by heterogeneities of frictional strength. The third regime is intermediate and develops areas of high slip that are much bigger than the local asperity size (self-affine properties of the slip distribution). This particular regime illustrates the possible misinterpretation of low frequency slip data (e.g. interferometric and GPS data) in terms of structural or compositional properties along the fault.

Spatio-temporal complexity of the rupture process and the earthquake activity have become an evidence with the increasing resolution of near field strong ground motion records. Sources have been shown to present large heterogeneities in the coseismic slip and the rupture velocity [*Archuleta*, 1984; *Brune*, 1991; *Cotton and Campillo*, 1995]. More recently, various combined inversions of interferometric, GPS and strong motion data have been used to better constrained the source tomography [*Wald*, 1996; *Hernandez et al.*, 1999; *Delouis et al.*, 2000]. Recent works (*Rubin et al.* [1999];*Nadeau et al.* [1995]) have shown also the existence of spatio-temporal correlations between micro-earthquakes occuring along creeping faults. The origin of this complexity is still poorly understood and often explained as generated by a combination of a static prestress field and fault structural or compositional heterogeneities. Whether the observed slip and slip rate patterns may reflect the underlying frictional or geometrical properties of the fault remains an important question. The goal of this work is to address, using a rather simple fault model, this hypothesis and to study the influence of quenched strength heterogeneities on the slip distribution of slow creeping faults.

We consider a simple scalar elastic model of the rupture along a fault plane, located at $y = 0$, within an unbounded homogeneous elastic solid assuming constant normal stress. The problem is governed by a scalar wave equation involving a two-dimensional displacement field $U(x, y; t)$ and a related shear traction $\sigma(x, y; t)$. The actual slip $u(x; t) = U(x, 0^+; t) - U(x, 0^-; t)$ is the slip discontinuity across the fault plane and $\tau(x; t)$ denotes the associated perturbation of traction. Since we focus on creeping faults, we assume that slip occurs quasi-statically and neglect any dynamical effects. In that case, we can neglect the radiation damping term and the stress change $\tau(x; t)$ due to variations of slip discontinuity along the fault is given by (e.g. [*Cochard and Rice*, 1997])

$$\tau(x; t) = \frac{\mu}{2\pi} PV \int_L J(x - \xi)[u(\xi; t) - u(x; t)]\, d\xi \qquad (1)$$

where integration takes place over the fault of size L and PV indicates the principal

value. The elastic kernel $J(x) = 1/x^2$ accounts for the long range elastic interactions and μ is the shear modulus. For plane strain, $u = u_x$, $\tau(x;t) = \sigma_{yx}(x,0;t)$ and $\alpha = 1-\nu$ while for anti-plane strain, $u = u_z$, $\tau(x;t) = \sigma_{yz}(x,0;t)$ and $\alpha = 1$. For simplicity, we assume an L periodic interface in the x direction such that the $1/x^2$ kernel in (1) transforms in $J_L(x) = (\pi/L)^2/\sin^2(\pi x/L)$.

To account for heterogeneous frictional properties along the interface, we balance $\tau(x;t)$ with a random quenched friction strength $\eta_p(x;u(x;t))$. We assume that strength fluctuations along the fault are strongly correlated over a scale a, and uncorrelated on larger scales. The scale a is assumed here to be small compared to the fault scale L ($L/a \ll 1$) and defines the scale of the fault asperities. In the remaining, the discretization length for the fault model will be chosen as the asperity scale a. Since we have assumed no spatial correlation between asperities, the friction strength $\eta_p(x;u(x;t))$ is assumed to have a uniform probability density over the interval $[\eta_c - \delta\eta_c; \eta_c + \delta\eta_c]$. For sake of simplicity, we set $a = 1$ (and any length scale of the problem is given in units of a).

It follows that, at any time, the quasi-static evolution motion of the fault has to satisfy:

$$\eta_p(x;u(x;t)) \geq \tau(x;t) \tag{2}$$

for all points x of the interface Γ. The evolution of the system may be regarded as purely dissipative, i.e. all the energy being used in frictional work [*Fisher*, 1998].

We assume that the fault is creeping at an arbitrary slow displacement rate so that only one asperity slips at a time allowing all the configurations of the slip distribution to be explored in the spirit of a Monte-Carlo simulation. At each step of the calculation, only the weakest point slips of an elementary distance s which defines the unit length in the direction of propagation. The fault evolves at imposed displacement and is characterized by the mean slip $\overline{u} = (1/L)\sum_{i=1}^{L} u_i$. Therefore the time t in equation (2) should be replaced by $\overline{u}$ which is the relevant variable for describing the evolution of

slip. However, time may be introduced by noting that the average slip $\overline{u}$ of the fault obeys $\overline{u} = V_0\, t$, where V_0 is the tectonic slip rate.

The weakest asperity x_{weak} corresponds to the site where the yield function Y (defined as the difference between frictional strength and shear traction) is minimum:

$$Y(x_{weak};\overline{u}) = \min_{\forall x \in \Gamma}[\eta_p(x; u(x;\overline{u})) - \tau(x;\overline{u})] \tag{3}$$

The asperities are supposed to experience new frictional properties after local slip (instantaneous healing) with $\eta_p(x_{weak}; u(x_{weak};\overline{u}))$ updated according to the uniform probability distribution. The asperity dislocation at x_{weak} induces, according to (1), a long range variation of the shear traction $\tau(x)$ along the fault. Then a new moving asperity is determined and the procedure is repeated again to explore successive equilibrium position of the fault.

The behavior of the system is controlled by the competition between local fluctuations of the frictional strength and the effect of long range elastic interactions. Using (1) the stress drop of a point that just slipped by an amount is s is $2\,\mu\, s/(\pi\, a)$. This allows to define a dimensionless parameter $\gamma = \mu\, s\sqrt{12}/(\pi\, a\, \delta\, \eta_c)$ where $2\,\delta\eta_c/\sqrt{12}$ is the rms of the frictional strength distribution.

When γ is much greater than 1, the elastic interactions screen the effect of the fluctuations of the frictional strengths. The heterogeneities are not strong enough to pin the front and slip can never be arrested. In our model for imposed displacement, the slip runaway is controlled, in contrast with a stress controlled boundary condition. For this pulse-like propagative regime, heterogeneities play a minor role and therefore this regime will be refered as the *weakly heterogeneous* (WH) regime.

When γ is much smaller than one, we observe an extreme regime where recurrent slip activity can occur at the same point since the stress drop due to elastic interactions is not big enough (compared to $\delta\eta_c$) to unload the point. This regime will be refered as the *strongly heterogeneous* regime (SH). In this case, the slip field is expected to have

the same statistical distribution than the fluctuations of the frictional strength, *e.g.* a white noise in the present study.

For the intermediate regime, the magnitude of the elastic interactions are of the order of the amplitude of the frictional strength variations. This is the *pining regime* (P) where interactions between frictional heterogeneities and elastic stress transfers lead to non trivial spatio-temporal correlations of slip in particular a self-affine scale invariance. Such a scale invariance is also observed for a crack front propagation [*Schmittbuhl and Måløy*, 1997].

Figure 1.

The simulations start with a zero displacement field. Figure 1 shows various slip distributions in steady state related to $\gamma = 10^{-4}$, 10^{-1} and 10^{3} illustrating the three regimes mentioned above.

In the P regime, the slip distribution reaches a stationary state which is relevant for mature creeping faults (*i.e.* faults which have undergone a sufficient amount of slip). Figure 1 for $\gamma = 0.1$ shows a typical slip distribution in the steady state regime: No characteristic length scale appears. The self-affine invariance of the slip fluctuations along the fault is characterized by the Hurst exponent ζ which can be estimated using the auto-correlation function $g(x, x'; \overline{u}) =< [(u(x; \overline{u}) - u(x'; \overline{u})]^2 >_x$ (where $< ... >_x$ means average over the whole fault). For a self-affine signal, the auto-correlation function behaves like a power law i.e. $g(x, x'; \overline{u}) \propto |x - x'|^{2\zeta}$ and implies $\delta u \propto \delta x^{\zeta}$ where $\delta u =< u(x + \delta x) - u(x) >_x$ represents the mean fluctuation of slip on the fault over a length δx. Many methods (variable bandwidth, return probability, Fourier spectrum, wavelet analysis, etc..., as discussed for instance in *Schmittbuhl et al.* [1995b]) may be used to measure ζ. For example the power spectrum $P(k)$ (i.e. Fourier transform of the auto-correlation function mentioned above) of a self affine signal with Hurst exponent ζ shows a power law behavior $P(k) \propto k^{-1-2\zeta}$. Using this last method, we found $\zeta \simeq 0.35$ a value consistent with previous estimates of ζ in similar models ([*Schmittbuhl et al.*, 1995a; *Schmittbuhl and Vilotte*, 1999]).

Figure 2.

We investigate space-time (where time should be understood as mean slip) in the stationary regime by studying the increment evolution between two states of the system separated by a slip $\Delta\overline{u}$. The evolution can be analyzed computing the power spectrum of the slip increment $\Delta u(x;\Delta\overline{u}) =< u(x;\overline{u}+\Delta\overline{u}) - u(x;\overline{u}) >_{\overline{u}}$ where $< ... >_{\overline{u}}$ means averaging over all the configurations $\overline{u}$. The power spectrum $P_{\Delta u}(k)$ of $\Delta u(x;\Delta\overline{u})$ is plotted in figure 2 for a system of size $L = 4096$ and various values of $\Delta\overline{u}$. For small increments $\Delta\overline{u}$, the spectrum is essentially flat showing that the spatial correlations between successive slip distributions occur at very short wavelengths. As $\Delta\overline{u}$ increases, the spectrum reaches a power law trend characteristic of self-affinity where correlations exist at all length scales. Self-affinity develops only over scales lower than a characteristic spatial scale $\xi(\Delta\overline{u})$ which defines an activity zone that spreads with the evolution of the slip increment $\Delta\overline{u}$ as (e.g. [*Tanguy et al.*, 1998])

$$\xi \propto \Delta\overline{u}^{1/z} \tag{4}$$

where z is a dynamic exponent. In the Fourier domain, the power spectrum should exhibit a power law trend for frequencies higher than $cste/\xi(\Delta\overline{u})$ and be flat for lower frequencies. This behavior is illustrated in figure 2. The spreading of the activity continues until the activity zone ξ reaches the system size L defining a characteristic slip increment $\Delta\overline{u}_L$. At that stage, the power spectrum will not evolve for slip greater than $\Delta\overline{u}_L$ since correlations have developed over the whole system size. The slope of the linear trend of the power spectra in figure 2 is -1.7, a value consistent with the self-affine scaling of $\overline{u}$ ($\xi \simeq 0.35$).

The spatial correlations of slip can be related to the temporal ones since $z = \zeta + 1$ (e.g. [*Tanguy et al.*, 1998]). After a slip increment $\Delta\overline{u}$, the activity is localized within a region of extension $\xi \propto \Delta\overline{u}^{1/z}$. The number of asperities that have slipped during that move is proportional to the slip area *i.e.* $\xi\Delta\overline{u} \propto \xi^{1+\zeta}$, where the relation $\Delta\overline{u} \propto \xi^{\zeta}$ has been used. The number of asperities is also proportional to the slip increment $\Delta\overline{u}$ so

that $\xi^{1+\zeta} \propto \xi^z$ giving the expected relation. **Figure 3.**

The spreading of the activity with increasing displacement in the P regime results from two competing effects: long range elastic interactions and frictional strength heterogeneities. The former tends to strongly correlate slip laterally while the latter tends to pin the slip at one site. Figure 3 shows the activity maps or locations of active sites as slip $\overline{u}$ is evolving for various values of the parameter γ ($\gamma = 10^{-4}$, 10^{-1} and 10^{3}).

In the propagative regime WH (top panel), the slip propagates laterally as observed in the zoom window. The size of the activity is expected to scale with displacement as $\xi \propto \overline{u}$ ($z = 1$) since the slip of an asperity triggers only the motion of its immediate neighbor.

In the strongly heterogeneous regime SH (middle panel of fig. 3), the activity is analogous to a brownian motion. The activity is spread all over the fault since the elastic coupling is too weak to overcome the frictional strength fluctuations. In this case, $\xi \propto \overline{u}^{1/2}$ ($z = 2$, $\zeta = -1/2$) as expected for a classical diffusive process. In the pining regime P (bottom panel), we observe a clustering of slip as shown within the zoom window of the activity map (fig. 3). We found $z \simeq 1.35$ as in *Schmittbuhl et al.* [1995a], a value bracketed by the $z = 1$ of the WH regime and the $z = 2$ of the SH regime. **Figure 4.**

We have studied so far spatial correlations of the asperity slips. At the scale of the fault, one can introduce a friction force $F_c(\overline{u})$ defined as $Y(x_{weak}; \overline{u})$ given in (3). $F_c(\overline{u})$ is the yield force above which the fault is moving. The energy (frictional work) dissipated by the fault after slip $\overline{u}$ is $W(\overline{u}) = \int_0^{\overline{u}} F_c(\lambda)\, d\lambda$. For the pinning regime P, the energy power spectrum $P_W(\omega)$ exhibits in figure 4 a power law scaling $W(\omega) \propto \omega^{-2}$. Such ω-square decay could be related to seismological observations of radiated spectrum for the far-field displacement [*Aki*, 1967; *Houston and Kanamori*, 1986].

We have studied a simple model of a creeping fault moving under a slow imposed displacement with long range elastic interactions and frictional heterogeneities. Three different regimes of slip fluctuations have been observed according to a non dimensional

parameter γ which compares elastic stress coupling and frictional strength fluctuations: a first regime ($\gamma \gg 1$) with a pulse-like propagation of the slip activity; an intermediate regime ($\gamma \simeq 1$) where the slip activity remains clustered over a characteristic length ξ, which results from the competition between long range elastic interactions and frictional strength fluctuations, and that evolves with the imposed displacement; a third regime ($\gamma \ll 1$) where activity spreads as a brownian motion and where slip fluctuations map frictional strength fluctuations.

The analysis may have interesting implications for interpretation of low frequency slip inversions using strong motion, GPS and SAR measurements. The slip fluctuations observed in our model should have a strong signature in GPS or SAR signals due to the power law decay of the slip power spectrum. Slip clusters of size ξ, as observed in the pinning regime (P), will appear at low frequencies as areas of uniform slip. In the light of the present analysis, slip patches inferred from GPS or SAR measurements may be quite misleading when mapped onto fault structural heterogeneities . Indeed, in the pinning regime the size of a slip activity zone is independent of the asperity size.

Acknowledgments. We are grateful to R. Madariaga, A. Cochard, and J. P. Ampuero for their generous help.

References

Aki, K., Scaling law of seimic spectrum, *J. Geophys. Res.*, *72*, 1217–1231, 1967.

Archuleta, R., A faulting model for the 1979 Imperial Valley, California earthquake, *J. Geophys. Res.*, *89*, 4559–4585, 1984.

Brune, J., Seismic source dynamics, radiation and stress, *Rev. Geophys.*, *29 Supplement*, 688–699, 1991.

Cochard, A., and J. R. Rice, A spectral method for numerical elastodynamic fracture analysis without spatial replication of the rupture event, *J. Mech. Phys. Solids*, *45*, 1393–1418, 1997.

Cotton, F., and M. Campillo, Inversion of strong ground motion in the frequency domain: Applications to 1992 Landers, California earthquake, *J. Geophys. Res.*, *100*, 3961–3975, 1995.

Delouis, B., J. Salichon, and D. Giardini, Joint inversion of InSAR and teleseismic data for the slip history of the Mw=7.4 Izmit (Turkey) earthquake, *Geophys. Res. Lett.*, submitted, 2000.

Fisher, D. S., Collective transport in random media: from superconductors to earthquakes, *Physics Reports*, *301*, 113–150, 1998.

Hernandez, B., F. Cotton, and M. Campillo, Contribution of radar interferometry to a two step inversion of the kinematic process of 1992 Landers Earthquake, *J. Geophys. Res.*, *104*, 13083–13100, 1999.

Houston, H., and H. Kanamori, Source spectra of great earthquake: teleseismic constraints on rupture process and strong motion, *Bull. Seismol. Soc. Am.*, *76*, 19–42, 1986.

Nadeau, R. M., W. Foxall, and T. V. McEvilly, Clustering and periodic recurrence of microearthquakes on the San Andreas fault at Parkfield, California, *Science*, *267*, 503–507, 1995.

Rubin, A. M., D. Gillard, and J.-L. Got, Microseismic lineations along creeping faults, *Nature*, *400*, 635–641, 1999.

Schmittbuhl, J., and K. Måløy, Direct observation of a self-affince crack propagation, *Phys. Rev. Lett.*, *78*, 3888–3891, 1997.

Schmittbuhl, J., and J. P. Vilotte, Interfacial crack front wandering: influence of quenched noise correlations, *Physica A*, *270*, 42–56, 1999.

Schmittbuhl, J., S. Roux, J. P. Vilotte, and K. J. Maløy, Interfacial crack pinning: Effect of nonlocal interactions, *Physical Review Letters*, *74*, 1787–1790, 1995a.

Schmittbuhl, J., J. P. Vilotte, and S. Roux, Reliability of self-affine measurements, *Physical Review E*, *51*, 131–147, 1995b.

Tanguy, A., M. Gounelle, and S. Roux, From individual to collective pinning: Effect of long-range elastic interactions, *Physical Review E*, *58*, 1577–1590, 1998.

Wald, D., Slip history of 1995 Kobe, Japan earthquake determined from strong motion teleseismic, and geodetic data, *J. Phys. Earth*, *44*, 489–504, 1996.

H. Perfettini, J. Schmittbuhl, Laboratoire de Géologie, Ecole Normale Supérieure, 75231 Paris Cedex 05, France. (e-mail: perfetti@geologie.ens.fr; schmittb@geologie.ens.fr)

J.P. Vilotte, Département de Sismologie UMR 7580 and Département de Modélisation Physique et Numérique, Institut de Physique du Globe de Paris, 4 Place Jussieu, 75252 Paris Cedex 05, France.

Received _____

This manuscript was prepared with AGU's LaTeX macros v4, with the extension package 'AGU^{++}' by P. W. Daly, version 1.6a from 1999/05/21.

Figure Captions

Figure 1. Examples of the slip pattern in the stationary regime for $L = 2048$ and $\gamma = 10^{-4}$, 0.1 and 10^3. Slip is normalized by its maximum value u_{max} over the fault. In the case $\gamma = 0.1$ no characteristic length is observed. Slip distribution exhibits a the self-affine scale invariance.

Figure 2. Power spectrum in the steady state regime of the incremental slip when $\gamma = 0.1$ for different increment displacements $\Delta\overline{u}$ and a system size of $L = 4096$. Starting from short range correlations, the system develops correlations at every length scales as $\Delta\overline{u}$ increases.

Figure 3. Activity maps for $L = 2048$ and different values of γ. (top) The regime WH ($\gamma = 10^3$) is dominated by the elastic interactions which results in a pulse-like propagation of slip. (middle) The intermediate regime P ($\gamma = 10^{-1}$) shows the existence of spatio-temporal correlations and the clustering of the activity. (bottom) regime SH ($\gamma = 10^{-4}$) is controlled by the fluctuations of the frictional strength and a random diffusion of the activity all through the fault.

Figure 4. Power spectrum of the large scale frictional work W for a system size $L = 4096$. The best fit has a slope -2 ($W(\omega) \propto \omega^{-2}$) leading to a scaling $W(\overline{u}) \propto \overline{u}^{1/2}$.

Figures

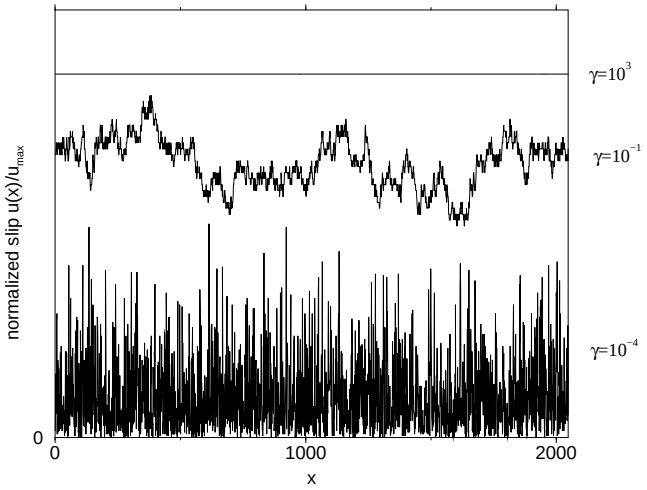

Figure 1. Examples of the slip pattern in the stationary regime for $L = 2048$ and $\gamma = 10^{-4}$, 0.1 and 10^3. Slip is normalized by its maximum value u_{max} over the fault. In the case $\gamma = 0.1$ no characteristic length is observed. Slip distribution exhibits a the self-affine scale invariance.

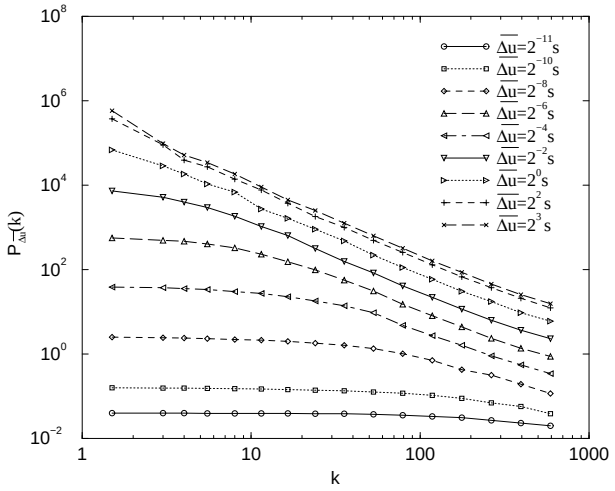

Figure 2. Power spectrum in the steady state regime of the incremental slip when $\gamma = 0.1$ for different increment displacements $\Delta\overline{u}$ and a system size of $L = 4096$. Starting from short range correlations, the system develops correlations at every length scales as $\Delta\overline{u}$ increases.

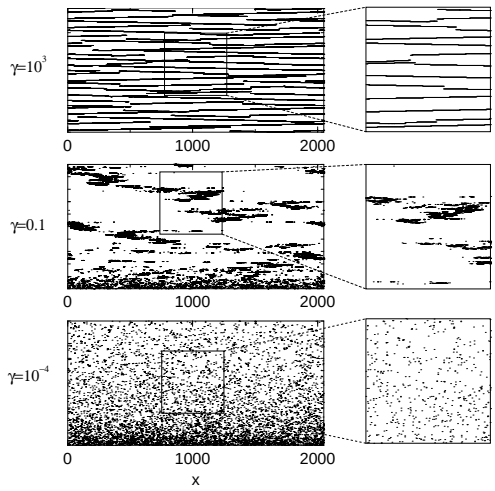

Figure 3. Activity maps for $L = 2048$ and different values of γ. (top) The regime WH ($\gamma = 10^3$) is dominated by the elastic interactions which results in a pulse-like propagation of slip. (middle) The intermediate regime P ($\gamma = 10^{-1}$) shows the existence of spatio-temporal correlations and the clustering of the activity. (bottom) regime SH ($\gamma = 10^{-4}$) is controlled by the fluctuations of the frictional strength and a random diffusion of the activity all through the fault.

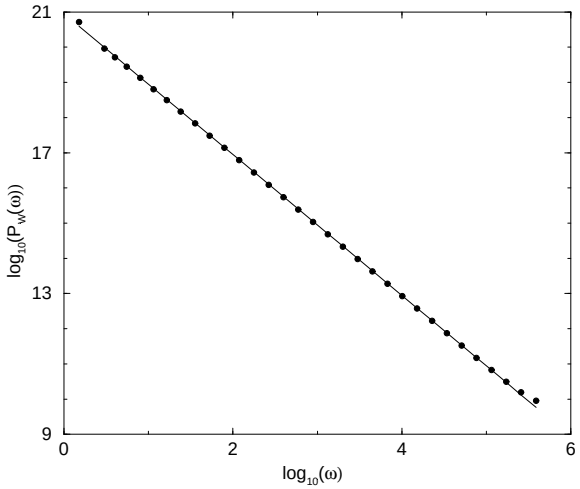

Figure 4. Power spectrum of the large scale frictional work W for a system size $L = 4096$. The best fit has a slope -2 ($W(\omega) \propto \omega^{-2}$) leading to a scaling $W(\overline{u}) \propto \overline{u}^{1/2}$.